Analysis of the dilepton invariant mass spectrum in C + C collisions at 2*A* and 1*A* GeV

M. Thomère,[1] C. Hartnack,[1] G. Wolf,[2] and J. Aichelin[1]

[1]*SUBATECH, Laboratoire de Physique Subatomique et des Technologies Associées, Université de Nantes, IN2P3/CNRS, Ecole des Mines de Nantes, 4 rue Alfred Kastler, F-44072 Nantes, Cedex 03, France*

[2]*KFKI, Post Office Box 49, H-1525 Budapest, Hungary*

(Received 31 January 2007; published 4 June 2007)

Recently the HADES Collaboration has published the invariant mass spectrum of e^+e^- pairs, $dN/dM_{e^+e^-}$, produced in C + C collisions at 2*A* GeV. Using electromagnetic probes, one hopes to get information from this experiment on hadron properties at high density and temperature. Simulations show that firm conclusions on possible in-medium modifications of meson properties will only be possible when the elementary meson production cross sections, especially in the *pn* channel, as well as production cross sections of baryonic resonances are better known. Presently one can conclude that (i) simulations overpredict by far the cross section at $M_{e^+e^-} \approx M_\omega^0$ if free production cross sections are used and that (ii) the upper limit of the η decay into e^+e^- is smaller than the present upper limit of the Particle Data Group. This is the result of simulations using the isospin quantum molecular dynamics approach.

DOI: 10.1103/PhysRevC.75.064902 PACS number(s): 25.75.−q, 24.10.Lx, 25.70.−z, 24.50.+g

I. INTRODUCTION

Theory has long predicted that the properties of hadrons change if they are surrounded by matter. For baryons this change has been verified in γA reactions where the total photon absorption cross section [1] shows a nontrivial dependence on the mass of the target nucleus. This nontrivial dependence has been interpreted as a change of the properties of the nuclear resonances in matter [2]. It is, however, difficult to asses whether the observed in-medium modifications have to be attributed to a change of the resonance properties or to a change of those of their decay products. Coupled channel calculations provide a means to answer this question, but presently the data are not sufficiently precise nor are the theoretical ingredients sufficiently well determined to allow for firm conclusions despite recent progress for some hadrons such as the ρ [3] and for K [4] mesons.

The strategy is different for the two cases. The study of the strange mesons takes advantage of the fact that they have to be produced in a heavy-ion reaction, that each strange hadron is accompanied by an antistrange one, and that the production cross sections are phase-space dominated. Systematic studies of the excitation function and of the system size dependence of the yields as well as of the modification of the measured K meson spectra as compared to that measured in *pp* collisions allow for conclusions on the interaction of the K mesons with the environment [5].

The ρ meson can decay into a dilepton pair, which—being an electromagnetic probe—no longer interacts with the nuclear environment. Therefore this dilepton pair carries direct information on the particle at the time point of its decay in the medium. The problem is that many resonances and mesons contribute to the dilepton yield and it is not easy to determine which particle is at the origin of the dilepton pair. To compare data with theory, one has to identify all dilepton sources and their contribution to the dilepton spectra. This superposition of the different sources is called a "cocktail plot." If it deviates from experiment at least one of the sources is not correctly described and one may start to test how this source is modified by the hadronic environment.

It was the DLS Collaboration who first presented dilepton invariant mass spectra in heavy-ion collisions at beam energies of around 1*A* GeV [6]. The systematic errors of these exploratory experiments have been, however, too large to allow for a detailed conclusion on the behavior of hadrons in matter. Later, at higher (SPS) energies, the CERES/NA45 Collaboration [7] presented spectra that were not in agreement with the standard cocktail plots. Two theoretical models have been advanced to explain this difference. Rapp and Wambach [3] calculated the in-medium modification of the spectral function of the ρ in hadronic matter. With this in-medium change of the spectral function the theoretical and experimental yields agree. As Eletsky *et al.* [8] explained ρ-meson and ρ-baryon interactions compensate each other as far as the shift of the pole mass is concerned, but collisions broaden the width considerably. Gallmeister *et al.* [9] showed that the discrepancy disappears as well if one adds to the spectrum the emission of the dileptons from a thermal $q\bar{q}$ (or hadron-hadron) annihilation using lowest order QCD calculations.

Most recently the NA60 Collaboration measured very precisely the invariant mass spectrum of dileptons in the ρ mass region [10] but it is still debated whether the discrepancy between cocktail plot and data is due to a modification of hadronic properties or due to annihilation processes. Additional information may be obtained from the p_t spectra [11] because each emission source shows a specific transverse momentum pattern. However, consensus on the relative importance of the different possible production mechanism has not been obtained yet.

To clarify this question it is necessary to study the dilepton production at lower energies where quarks remain bound in hadrons and hadron-hadron annihilations are rare. Then the process proposed by Gallmeister is absent and thermal production does not play a decisive role. In addition, one has to investigate small systems where direct

collisions dominate over the production in the participant heat bath.

Recently, the HADES Collaboration has published the dilepton invariant mass spectrum for the reaction C + C at 2*A* GeV [12]. This system is small and at this energy the formation of a quark phase is beyond reach, as the analysis of many other observables has shown. It may therefore serve to solve the question of how the ρ meson changes in a hadronic environment provided that it can be proven that all the other ingredients of the cocktail plot are well under control.

It is the purpose of this article to investigate in detail the dilepton invariant mass spectra by using one of the presently available programs that simulate heavy-ion reactions on an event-by-event basis, the isospin quantum molecular dynamics (IQMD) approach. The main objective is to find out whether the present dilepton data are sufficiently precise to allow for conclusions on the theoretically predicted change of the particle properties in a nuclear environment or to identify the obstacles on the way to achieve this goal. We concentrate in this exploratory study on the most significant modifications: mass shifts and changes of the decay width.

Before we present the results of our simulations we start with a short presentation of the model and a discussion of our present theoretical and experimental knowledge on all the elementary processes that contribute to the dilepton spectra and of how they are implemented in our simulation program.

II. THE IQMD MODEL

The semiclassical IQMD program [13] simulates heavy-ion reactions on a event-by-event basis and is one of the standard analyzing tools for heavy-ion reactions at and below 2*A* GeV. In this program hadrons interact by potentials and by collisions. The former ones are Brückner G-matrix parametrizations for the baryons or parametrized meson-baryon potentials. Thus nuclei are bound objects with a binding energy following the Weizsäcker mass formula. If two hadrons come closer than $r = \sqrt{\sigma_{\mathrm{tot}}/\pi}$ they collide. If several exit channels are available a random number determines which one is realized. The relative weight is given by the relative cross section. The momenta and the mass (if the particles have a finite width) of the hadrons in the final state are randomly determined. Their distribution follows either experimental measurements or phase space, if experimental results are not available. In the standard version [13] of the program, nucleons as well as baryonic resonances, pions, and kaons are the particles that are propagated.

For the investigation presented here we have added production cross sections of all particles that might contribute to the invariant mass spectrum of dileptons: np bremsstrahlung, η Dalitz and direct decay, ω (Dalitz and direct) and ρ decay, Δ Dalitz decay, and π^0 Dalitz decay. Because we concentrate on a very light system, where the probability that mesons have secondary interactions is small, it has not been necessary to add the (largely unknown) meson absorption or rescattering cross sections or to use off-shell transport approaches. When these particles are produced we use the branching ratios of the Particle Data Group [14] to determine their contribution to the dilepton spectrum.

III. ELEMENTARY DILEPTON CROSS SECTIONS

A. π^0 production and decay

At low invariant mass the overwhelming number of dileptons comes from the decay of π^0 mesons, which can decay into dileptons via $\pi^0 \to e^+e^-\gamma$. The shape of the mass distribution of a dilepton in a π^0 Dalitz decay is given by [15]

$$\frac{dN}{dM} = \frac{1}{M}\left(1+2\frac{m_{e^-}^2}{M^2}\right)\left(1-\frac{M^2}{m_{\pi_0}^2}\right)^3\sqrt{1-4\frac{m_{e^-}^2}{M^2}}, \quad (1)$$

where m_{π_0} is the mass of the π_0, m_{e^-} is the electron mass, and M is the mass of the dilepton pair. We take the branching ratio BR($\pi^0 \to e^+e^-\gamma$) as 0.01198.

B. η production and decay

In the energy regime of interest here, the η production in pp collisions has been well studied by the TAPS [16] and the DISTO Collaborations [17]. This can be seen in Fig. 1, which

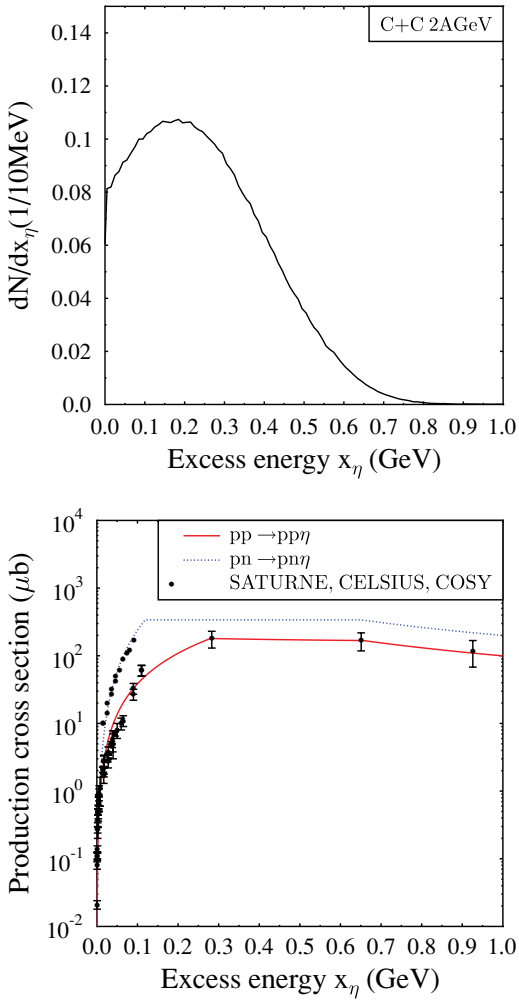

FIG. 1. (Color online) (Top) Excess energy (x_η) distribution of NN collisions in the C + C reaction at 2*A* GeV. (Bottom) Production cross section of the η meson. The solid curves are fits [Eq. (3)] to the data [16,19].

shows on top the distribution of the η excess energies in the nucleon-nucleon (NN) collisions for the reaction C + C at $2A$ GeV. The excess energy x_η is defined as

$$x_\eta = \sqrt{s} - 2M_N - M_\eta \,. \tag{2}$$

We see that excess energies below 0.6 GeV are most relevant for this reaction. In the bottom part of Fig. 1 we display the world data points for η production in elementary NN collisions [16–18]. Whereas the cross section $\sigma(pp \to pp\eta)$ is known over the whole excess energy interval of relevance for our investigation, the $\sigma(pn \to pn\eta)$ cross section is known only up to an excess energy of $x_\eta = 0.12$ GeV. Thus we have to extrapolate this cross section into the relevant excess energy domain. This extrapolation leaves a lot of freedom even if the η meson production cross section has been measured in heavy-ion reactions by the TAPS Collaboration. This is because in heavy-ion reactions a multitude of processes may modify the elementary cross section at the same nominal energy. These processes and the consequences will be discussed later. We parametrize the $\sigma(pn \to pn\eta)$ and $\sigma(pp \to pp\eta)$ cross section by a fit using the form

$$\sigma(x_\eta) = a x_\eta^b \,, \tag{3}$$

with $a = 1213.8$, $a = 162.1$, $a = 99.6$ μb and $b = 1.50$, $b = -0.08$, $b = -1.24$ for excess energies of $x_\eta < 283$ MeV, $283 < x_\eta < 651$ MeV, $x_\eta > 651$ MeV for pp collisions and $a = 25623$, $a = 324.3$, $a = 199$ μb and $b = 2.03$, $b = -0.08$, $b = -1.24$ for excess energies of $x_\eta < 200$ MeV, 200 MeV $< x_\eta < 651$ MeV, $x_\eta > 651$ MeV for np collisions assuming that at large excess energies the np cross section is twice the pp cross section. These fits are also displayed in Fig. 1.

We parametrize the shape of the mass distribution of the η by [20]

$$\frac{dN}{dM} = \frac{\left(1 + 2\frac{m_{e^-}^2}{M^2}\right)\sqrt{1 - 4\frac{m_{e^-}^2}{M^2}}}{\left(m_\eta^2 - M^2\right)^2 + \left[m_\eta \left(\frac{\Gamma_\eta m_\eta}{M} \frac{\left(M^2/4 - m_{e^-}^2\right)^{3/2}}{\left(m_\eta^2/4 - m_{e^-}^2\right)^{3/2}}\right)\right]^2} \,, \tag{4}$$

with $m_\eta = 0.547$ GeV and $\Gamma_\eta = 1.18$ keV.

1. Contribution of the N*(1535)

The very detailed experimental investigation of η production in pp collisions at excess energies of 324, 412, and 554 MeV (corresponding to beam energies of $E_{\text{beam}} = 2.15$, 2.5, and 2.85 GeV) by the DISTO Collaboration [17] allows us to identify the different production channels by analyzing the $p\eta$ invariant mass spectrum. As predicted by theory [21,22], there are essentially two channels, a direct production channel and a production via the $N^*(1535)$ resonance. The direct contribution follows the three-body phase space for the $pp \to pp\eta$ reaction. The experimental mass distribution of the $N^*(1535)$ resonance created in the reaction $pp \to N^*(1535)p$ can be described by a Breit-Wigner distribution of the form [17]

$$\sigma(M) = \frac{A M_R^2 \Gamma_R^2}{\left(M_R^2 - M^2\right)^2 + M_R^2 \Gamma_R^2 x^2(M, M_R)} \,, \tag{5}$$

with

$$x(M, M_R) = b_\eta \frac{q_\eta(M)}{q_\eta(M_R)} + b_\pi \frac{q_\pi(M)}{q_\pi(M_R)} \,, \tag{6}$$

where b_η is the branching ratio of the decay $N^*(1535) \to N\eta$ (which we assume to be 55%) and b_π is the branching ratio of the decay $N^*(1535) \to N\pi$ (which counts for 45%). The terms q_π and q_η are the momenta of π and η in the frame of the resonance and are given by

$$q_\eta(M_{N^*}) = \sqrt{\left(\frac{M_{N^*}^2 - M_p^2 + M_\eta^2}{2M_{N^*}}\right)^2 - M_\eta^2} \tag{7}$$

and

$$q_\pi(M_{N^*}) = \sqrt{\left(\frac{M_{N^*}^2 - M_p^2 + M_\pi^2}{2M_{N^*}}\right)^2 - M_\pi^2} . \tag{8}$$

We note in passing that in Ref. [17] the square on the x in Eq. (5) has been omitted. In Fig. 2 we display for the three energies that have been measured by the DISTO Collaboration [17], the total experimental and theoretical $p\eta$ invariant mass distribution, and the different contributions to the theoretical curve. The experimental data are best reproduced for $M_R = 1.530$ GeV and $\Gamma_R = 150$ MeV. As expected, the $N^*(1535)$ resonance enhances the low invariant mass part as compared to phase space.

How the resonance production modifies the spectra of protons and η's as compared to the production according to the three-body phase space is shown in Fig. 3. On the left-hand side we display the center-of-mass momentum of the η; on the right-hand side the proton momentum in the pp rest frame is shown. Choosing these variables allows for a comparison with the experimental results. We see clearly the consequence of η resonance production and therefore it will be difficult to separate the modification of the η in the medium from that of the $N^*(1535)$ resonance. Both will show up as a modification of the dilepton spectra.

2. η decay into dileptons

With a branching ratio of 6×10^{-3} [14] the η decays into $e^+e^-\gamma$. The shape of the invariant mass distribution of the dilepton pair is given by [15]

$$\frac{dN}{dM} = \frac{1}{M}\left(1 + 2\frac{m_{e^-}^2}{M^2}\right)\left(1 - \frac{M^2}{m_\eta^2}\right)^3 \sqrt{1 - 4\frac{m_{e^-}^2}{M^2}} \,, \tag{9}$$

where m_η is the mass of the η, m_{e^-} is the electron mass, and M is the mass of the dilepton pair. It has been shown that this expression has to be multiplied by an electromagnetic form factor. With

$$\left(\frac{dN}{dM}\right)_{\text{tot}} = F(M^2)^* \frac{dN}{dM} \,, \tag{10}$$

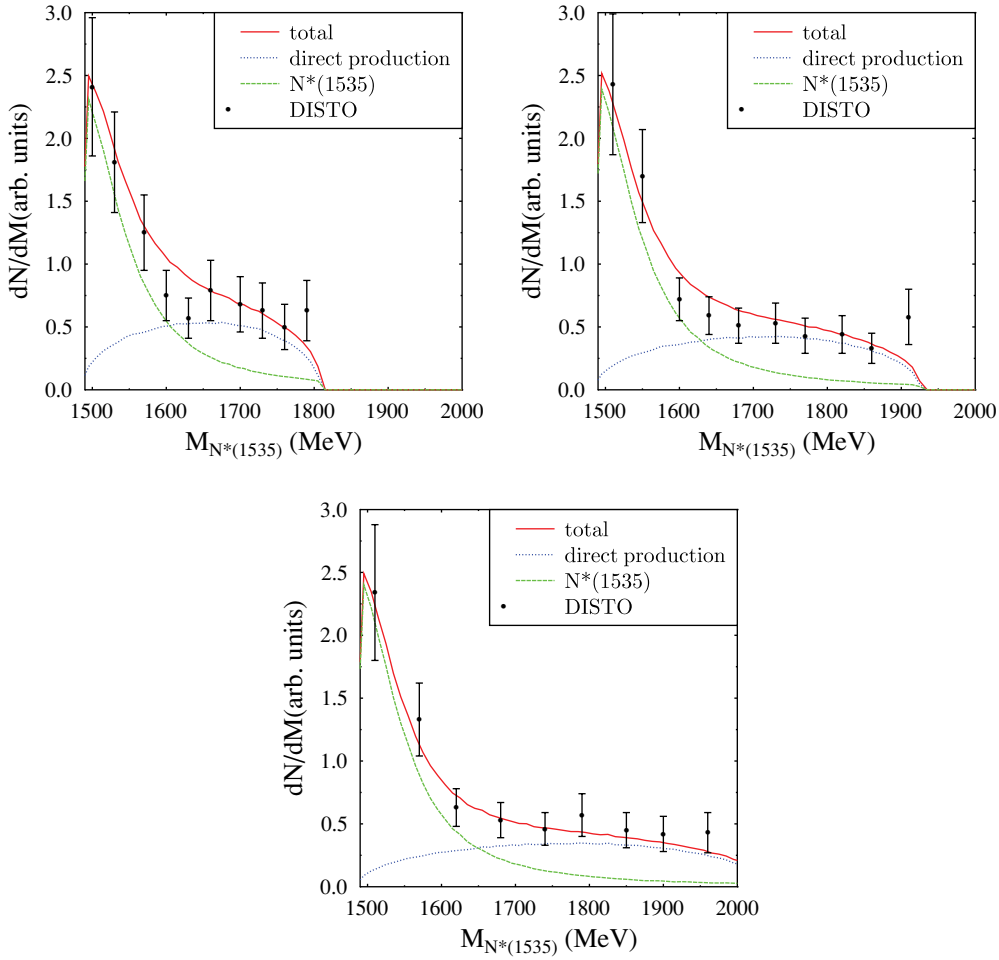

FIG. 2. (Color online) Simulated invariant mass spectrum of the outgoing proton and the η meson in the $pp \to pp\eta$ reaction for three beam energies (2.15, 2.5, and 2.85 GeV). The curves represent the sum of the contributions from the two productions channels of the η, the direct production, and that via the $N^*(1535)$ resonance. The data [17] have no absolute normalization. We normalize them here to our result at $M_{N^*(1535)} = 1500\ \mathrm{MeV}/c^2$.

where

$$F(M^2) = \left(\frac{1}{1 - \frac{M^2}{\Lambda_\eta^2}}\right)^2 \tag{11}$$

with $\Lambda_\eta = (0.72 \pm 0.09)$ GeV, one finds good agreement with data [20]. In addition to the three-body decay there may also be a two-body one into a dilepton pair. The Particle Data Group [14] quotes as an upper limit a branching ratio of 7.7×10^{-5}. We include this value in our standard calculation (which will be explained later).

C. ω production and decay

The ω production in pp collisions for excess energies below 440 MeV has been studied at COSY [23], at SATURNE [24], and by the DISTO [25] Collaboration. The cross section as well as our fit of the form $a{x_\omega}^b$, where x_ω is the excess energy in millions of electron volts, $a = (192.204 \pm 8.622)$ μb, and $b = 1.12182 \pm 0.1077$, is shown in Fig. 4. We include in our simulation as well the endothermic ($\sqrt{s_0} \simeq m_\omega - m_\pi = 643$ MeV) reaction $\pi + N \to \omega + N$. Because π's have usually only a small energy this reaction is less important than the baryonic channel. The experimental data have been parametrized [26] by

$$\sigma_{\pi N \to \omega N}(\mathrm{mb}) = \frac{1.38(\sqrt{s} - \sqrt{s_0})^{1.6}}{0.0011 + (\sqrt{s} - \sqrt{s_0})^{1.7}}, \tag{12}$$

with σ in milibarns and $\sqrt{s}$ and $\sqrt{s_0}$ in billions of electron volts. The term $\sqrt{s_0} = m_N + m_\omega$ (1.721 GeV for the ω in vacuum) is the threshold energy. It has been suggested that the production of the ω passes by the excitation of baryon resonances [27,28] where the $N^*(1535)$ plays a prominent role having a substantial branching ratio into the $N\omega$ channel [29–31]. It produces ω mesons with masses well below 783 MeV. If this were the case the strong ωN coupling would lead to a strong off-shell contribution to $d\sigma/dM$ (with M being the invariant mass of the dilepton pair) at invariant masses well below the free ω mass peak. This off-shell ω production would even dominate the dilepton spectra up to excess energies of several hundred MeV. Only very recently have calculations of

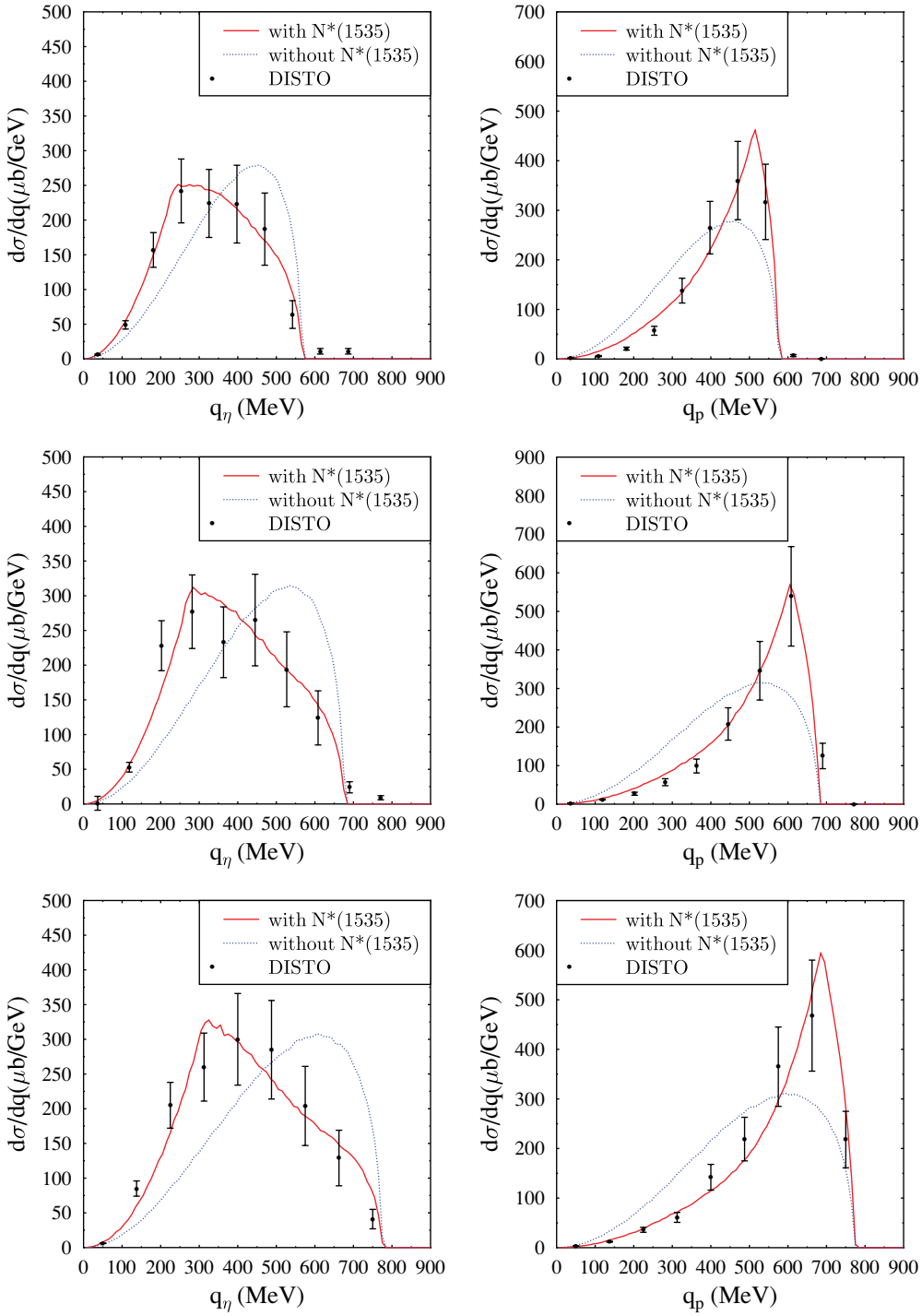

FIG. 3. (Color online) Differential cross section in IQMD as a function of the center-of-mass momentum of the η meson (left) and as a function of the proton momentum in the pp rest system (right) for $pp \to pp\eta$ collisions at different beam energies, $E_{\text{beam}} = 2.15$ GeV (top), $E_{\text{beam}} = 2.5$ GeV (middle), and $E_{\text{beam}} = 2.85$ GeV (bottom). Solid lines represent η production including the contribution of the $N^*(1535)$ resonance and dashed curves represent the direct production via a uniform three-body phase space distribution. The experimental data are from Ref. [17].

the spectral function been advanced to exploit the available γN and πN data in a coupled channel analysis [30,32].

A $\gamma A \to \omega$ experiment was recently performed by the CBELSA/TAPS Collaboration, who observed that the pole mass decreases with increasing density of the environment. [33]. For momenta less than 500 MeV/c^2, they observed an ω pole mass of $M = [722^{+2}_{-2}(\text{stat})^{+35}_{-5}(\text{syst})]$ MeV/c^2 for an average density of $0.6\rho_0$. Unfortunately, no significant measurement of the width was obtained owing to the dominance of the experimental resolution. Using thess data and

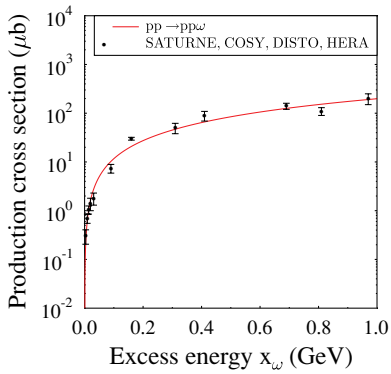

FIG. 4. (Color online) Production cross section of the ω in pp collisions up to an excess energy of 440 MeV and our fit of the form $\sigma = a x_\omega^b$. The data are from Refs. [23–25].

the Brown-Rho scaling formula

$$m_\omega^* = m_\omega^0 \left(1 - \alpha \frac{\rho}{\rho_0}\right) \tag{13}$$

we find $\alpha = 0.13$. Figure 5 shows the density distribution at the ω production points for a C + C collision at 2A GeV. The average density of $\langle\rho\rangle = 1.394\rho_0$ is twice that for the TAPS experiment. Applying Eq. (2) we obtain a wide distribution around the average pole mass of $M = 641$ MeV.

In our simulation we have the option to use this in-medium mass modification. Because there are no conclusive results on the width we kept the free value of 8 MeV. The shape of the invariant mass distribution of dileptons from the ω decay is given by the Breit-Wigner distribution,

$$\frac{dN}{dM} = \frac{\left(1 + 2\frac{m_{e^-}^2}{M^2}\right)\sqrt{1 - 4\frac{m_{e^-}^2}{M^2}}}{\left(m_\omega^2 - M^2\right)^2 + \left[m_\omega\left(\frac{\Gamma_\omega m_\omega}{M}\frac{\left(M^2/4 - m_{e^-}^2\right)^{3/2}}{\left(m_\omega^2/4 - m_{e^-}^2\right)^{3/2}}\right)\right]^2}, \tag{14}$$

with $\Gamma_\omega = 8$ MeV and m_ω as defined in Eq. (13).

Another uncertainty is the production of the ω in pn reactions. In meson exchange models the relative strength of the production in pp and pn reactions depends strongly on the

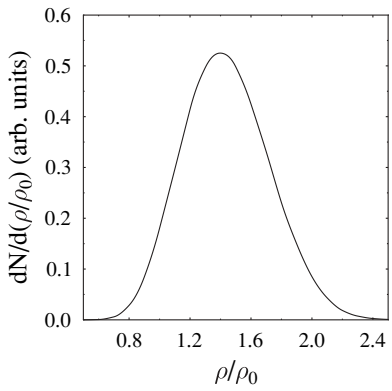

FIG. 5. Distribution of the density at the ω production points in units of the normal nuclear matter density ρ_0 for the reaction C + C at 2A GeV.

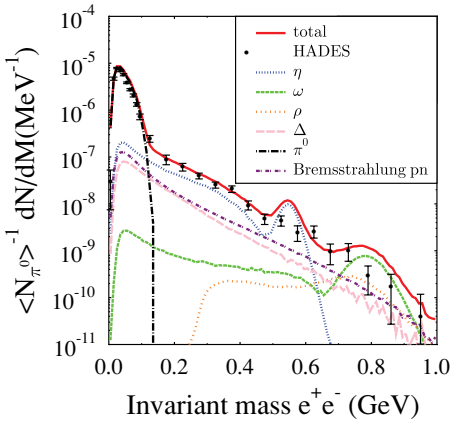

FIG. 6. (Color online) The invariant mass spectrum of the HADES Collaboration as compared with IQMD simulations for C + C at 2A GeV using $\sigma(np \to np\eta) = 2\sigma(pp \to pp\eta)$, $\sigma(np \to np\omega) = 5\sigma(pp \to \omega)$, $M_\omega = M_\omega^0$, and the branching ratio $(\eta \to e^+e^-) = 7.7 \times 10^{-5}$ (model A).

quantum number of the exchanged mesons. Neglecting possible differences owing to initial and final state interactions, we expect $\sigma(pn \to pn\omega)/\sigma(pp \to pp\omega) = 5$, if only isovector mesons (π, ρ) are exchanged [34]. The two data points for the reaction $np \to d\omega$ point toward an enhancement of the pn cross section as compared to the pp cross section [34]. The error bars are, however, too large to quantify this enhancement. In our simulations we assume $\sigma(pn \to pn\omega) = b * \sigma(pp \to pp\omega)$ with different values of b.

The ω contributes to the dilepton spectrum in two different ways. Either it decays directly into a dilepton pair whose invariant mass equals that of the ω meson or the dilepton pair is accompanied by a π_0 meson. For the latter channel the shape of the dilepton invariant mass distribution has been

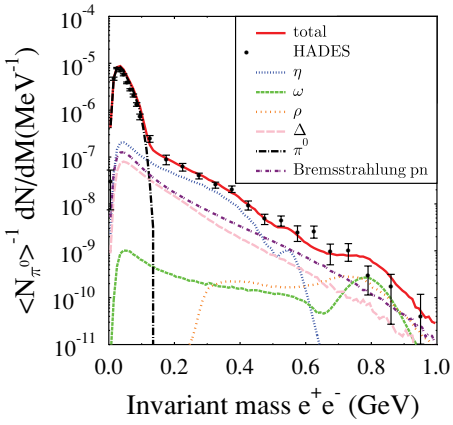

FIG. 7. (Color online) The invariant mass spectrum of the HADES Collaboration as compared with IQMD simulations for C + C at 2A GeV using $\sigma(np \to np\eta) = 2\sigma(pp \to pp\eta)$, $\sigma(np \to np\omega) = \sigma(pp \to pp\omega)$, $M_\omega = M_\omega^0$, and the branching ratio $(\eta \to e^+e^-) = 7.7 \times 10^{-6}$ (model B).

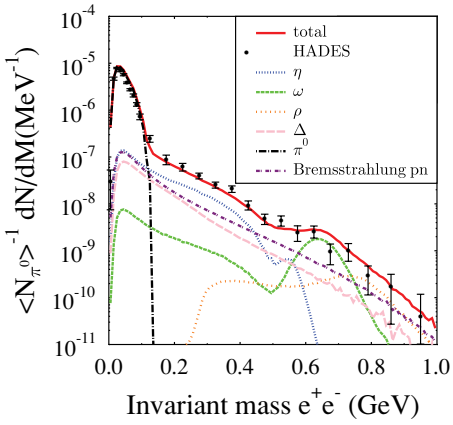

FIG. 8. (Color online) The invariant mass spectrum of the HADES Collaboration as compared with IQMD simulations for C + C at 2A GeV using $\sigma(np \to np\eta) = 2\sigma(pp \to pp\eta)$, $\sigma(np \to np\omega) = 5\sigma(pp \to pp\omega)$, $M_\omega = M_\omega^0(1 - 0.13\rho/\rho_0)$, and the branching ratio $(\eta \to e^+e^-) = 7.7 \times 10^{-6}$ (model C).

parametrized by Kroll and Wada [15] as

$$\frac{dN}{dM} = \frac{1}{M}\left(1 + 2\frac{m_{e^-}^2}{M^2}\right)\left[\left(1 + \frac{M^2}{m_\omega^2 - m_{\pi^0}^2}\right)^2 - 4\frac{m_\omega^2 M^2}{\left(m_\omega^2 - m_{\pi^0}^2\right)^2}\right]^{3/2}\sqrt{1 - 4\frac{m_{e^-}^2}{M^2}}\,, \tag{15}$$

where M is the invariant dilepton mass. This Dalitz-type decay has to be corrected by an electromagnetic form factor [20]:

$$\left(\frac{dN}{dM}\right)_{\text{tot}} = F(M^2)^* \frac{dN}{dM}\,, \tag{16}$$

with

$$F(M^2) = \frac{a^4}{(a^2 - M^2)^2 + a^2 b^2}\,, \tag{17}$$

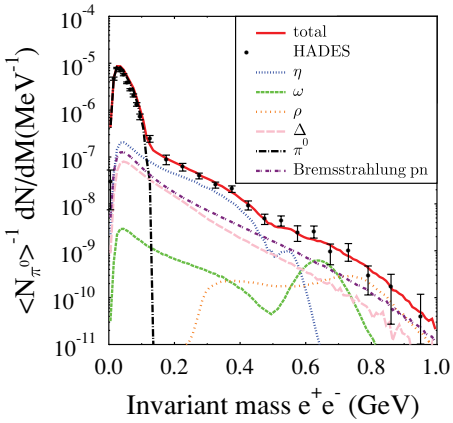

FIG. 9. (Color online) The invariant mass spectrum of the HADES Collaboration as compared with IQMD simulations for C + C at 2A GeV using $\sigma(np \to np\eta) = 2\sigma(pp \to pp\eta)$, $\sigma(np \to np\omega) = \sigma(pp \to pp\omega)$, $M_\omega = M_\omega^0(1 - 0.13\rho/\rho_0)$, and the branching ratio $(\eta \to e^+e^-) = 7.7 \times 10^{-6}$ (model E).

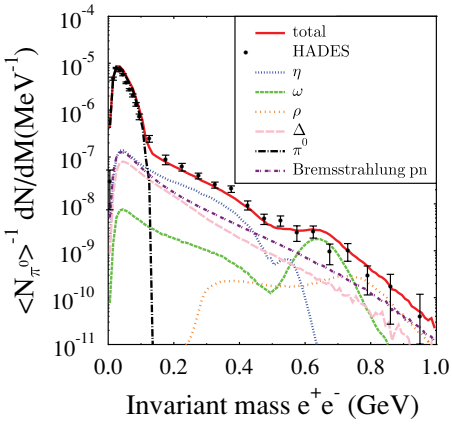

FIG. 10. (Color online) The invariant mass spectrum of the HADES Collaboration as compared with IQMD simulations for C + C at 2A GeV using $\sigma(np \to np\eta) = \sigma(pp \to pp\eta)$, $\sigma(np \to np\omega) = 5\sigma(pp \to pp\omega)$, $M_\omega = M_\omega^0(1 - 0.13\rho/\rho_0)$, and the branching ratio $(\eta \to e^+e^-) = 7.7 \times 10^{-6}$ (model D).

and $a = 0.6519$ GeV, $b = 0.04198$ GeV to be in agreement with data. The branching ratios into the two channels are given by 5.9×10^{-4} (7.14×10^{-5}) for the $e^+e^-\pi$ (e^+e^-) channel [14]. Both the unknown pn cross section as well as the little known off-shell contribution at small excess energies make it difficult to predict the ω contribution at invariant dilepton masses between 0.6 and 0.8 GeV.

D. ρ production and decay

In our simulation the ρ meson can be produced in three channels: $NN \to NN\rho$, $\pi N \to \rho N$, and $\pi^+\pi^- \to \rho$.

The few experimental data points of the total cross section in the $NN \to NN\rho$ channel have been fitted by [35]

$$\sigma_{NN\to NN\rho}(\text{mb}) = \frac{0.24(\sqrt{s} - \sqrt{s_0})}{1.4 + (\sqrt{s} - \sqrt{s_0})^2}\,, \tag{18}$$

with $\sqrt{s_0} = 2.646$ GeV being the threshold of the reaction. In view of the strong coupling of the ρ to nuclear resonances

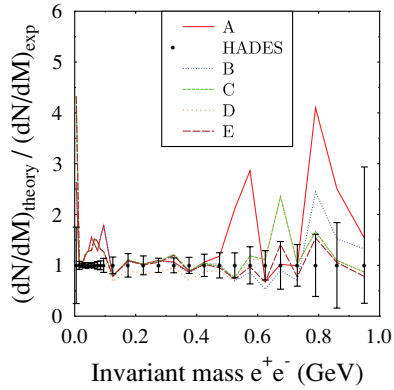

FIG. 11. (Color online) Invariant mass dependence of the ratio theory/experiment for the C + C reaction at 2A GeV for the different parametrizations of unknown physical input quantities (see Table I for details)

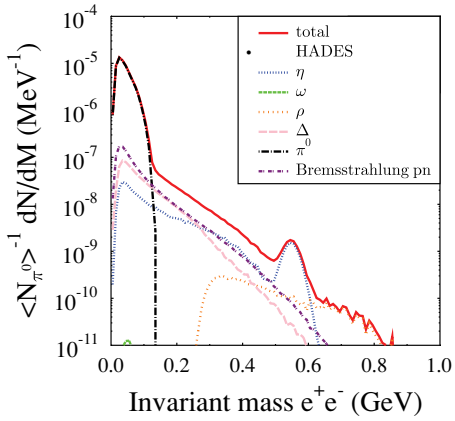

FIG. 12. (Color online) The invariant mass spectrum of IQMD simulations for C + C at 1A GeV using $\sigma(np \to np\eta) = 2\sigma(pp \to pp\eta)$, $\sigma(np \to np\omega) = 5\sigma(pp \to pp\omega)$, $M_\omega = M^0_\omega$, and the branching ratio $(\eta \to e^+e^-) = 7.7 \times 10^{-5}$.

this course-grained parametrization has most probably large systematic errors and presents a lower limit to the ρ production. Other models such as URQMD use a parametrization of the resonance production that yields higher ρ yields. For the $\pi + N \to N + \rho$ data [30] we use the parametrization of [26]

$$\sigma_{\pi N \to \rho N}(\text{mb}) = \frac{1.5(\sqrt{s} - \sqrt{s_0})^{2.2}}{0.0018 + (\sqrt{s} - \sqrt{s_0})^{3.5}}, \qquad (19)$$

with $\sqrt{s_0} = 1.708$ GeV.

Having a large width and therefore a short lifetime, the ρ meson is an ideal particle to probe whether the nuclear environment changes mesonic properties. If produced in hadronic matter the majority of them decay in matter and therefore the dileptons carry direct information on the in-medium properties. Theory predicts that these properties are different from that of the free ρ. Whereas there now seems to be consensus that the width of the ρ increases if brought into a nuclear environment [3,36,37], the question of how the

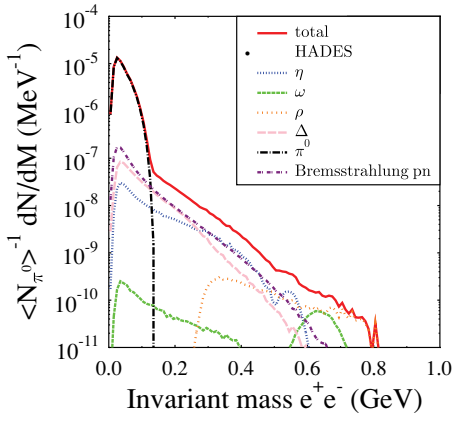

FIG. 13. (Color online) The invariant mass spectrum of IQMD simulations for C + C at 1A GeV using $\sigma(np \to np\eta) = 2\sigma(pp \to pp\eta)$, $\sigma(np \to np\omega) = 5\sigma(pp \to pp\omega)$, $M_\omega = M^0_\omega(1 - 0.13\rho/\rho_0)$, and the branching ratio $(\eta \to e^+e^-) = 7.7 \times 10^{-6}$.

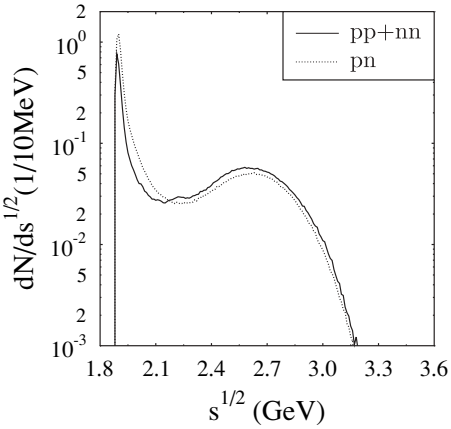

FIG. 14. Distribution of $\sqrt{s}$ of NN collisions in a C + C reaction at 2A GeV.

pole mass changes is still debated. Based on QCD sum rule calculations, Hatsuda and Lee [38] predicted a lowering of the ρ mass in a nuclear environment, a suggestion that has later been confirmed by Brown and co-workers [39,40]. More recent and more sophisticated calculations leave, in contrast, the ρ mass almost unchanged [3,8,37]. Experimentally the situation is also far from being clear. In pA collisions [41] at 12 GeV a decrease of the mass $[m(\rho)/m(0) = 1 - 0.09\rho/\rho_0$—about half the value predicted by theory] and no increase of the width have been reported. The dilepton data in In + In collisions at 158 A GeV [10] are best described by using the free ρ pole mass but a considerable broadening of the mass distribution. In contradiction to the earlier theoretical expectations this broadening is almost symmetric around the pole mass, but recently it has been pointed out [42] that the Φ-functional approach may explain this symmetry.

Whether these experimental differences are exclusively due to the different environments (cold nuclear matter in pA reactions and an expanding meson-dominated fireball after a possible phase transition from a quark gluon plasma in AA collisions) has not been fully explored yet. It is very difficult to exploit this experimental information for heavy-ion reactions at 2A GeV where theory predicts that most of the ρ mesons

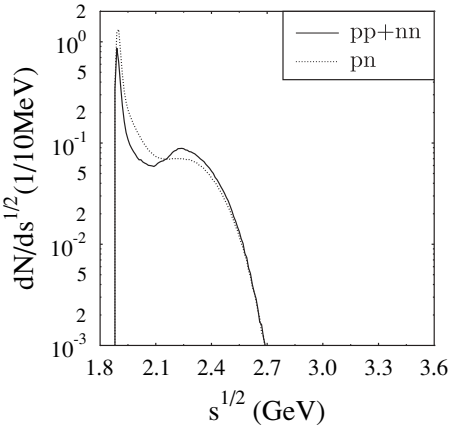

FIG. 15. Distribution of $\sqrt{s}$ of NN collisions in a C + C reaction at 1A GeV.

are decay products from nuclear resonances, especially of the $N^*(1520)$ resonance, which has a branching ratio of 15–25% into the ρN channel. For the present status of the theoretical spectral function calculations for the ρ meson we refer to Refs. [32,43].

For the ω meson, the inconclusive situation of theory and experiment suggests employing for this exploratory study the free pole mass distribution of the ρ:

$$\frac{dN}{dM} = \frac{m_\rho^2}{\left(\frac{M^2-m_{\rho_2}^2}{m_\rho}\right)^2 + \Gamma_\rho^2}, \tag{20}$$

with $m_\rho = 0.775$ GeV/c^2, $m_{\rho_2} = 0.761$ GeV/c^2, $\Gamma_\rho = 0.118$ GeV/c^2 [44], and the parametrized free cross sections. For the branching ratio of the ρ into dileptons we use 4.5×10^{-5}.

E. *pn* bremsstrahlung

In each np collision real and virtual photons can be produced. The invariant mass distribution of the e^+e^- pairs, the decay product of the virtual photon, is given by

$$\frac{dP(s,M)}{dM} = \frac{1}{3}\frac{\alpha^2}{\pi^2}\frac{1}{M}\frac{s-(m_p+m_n)^2}{e_{\rm cm}^2} \times \ln\left(\frac{q_{\rm max}+q_{0\rm max}}{M} - \frac{q_{\rm max}}{q_{0\rm max}}\right), \tag{21}$$

with

$$q_{0\rm max} = \frac{s+M^2-(m_p+m_n)^2}{2\sqrt{s}} \tag{22}$$

and

$$q_{\rm max} = \sqrt{q_{0\rm max}^2 - M^2}. \tag{23}$$

Here $\sqrt{s}$ is the np center-of-mass energy, $e_{\rm cm}$ is the energy of the incoming proton in the np center-of-mass system, α is the electromagnetic coupling constant, m_p and m_n are the masses of the proton and the neutron, respectively, $q_{0\rm max}$ is the maximal dilepton energy, and $q_{\rm max}$ is the maximal dilepton momentum. The bremsstrahlung from pp collisions is of quadrupole type and can be neglected as compared to the dipole pn bremsstrahlung.

F. Δ Dalitz decay

It is not experimentally verified yet whether the Dalitz decay into e^+e^- of the Δ resonance exists but since it decays into a photon it should also decay into a dilepton. The width of the Dalitz decay to dileptons of invariant mass M is determined by QED [45]:

$$\frac{d\Gamma}{dM^2} = \frac{\alpha}{3\pi}\frac{\Gamma_0(M^2)}{M^2}, \tag{24}$$

where

$$\Gamma_0(M^2) = \frac{\lambda^{1/2}\left(M^2, m_N^2, m_\Delta^2\right)}{16\pi m_\Delta^2} m_N [2M_t(M^2) + M_l(M^2)] \tag{25}$$

is the total decay rate into a virtual photon with mass M and

$$\lambda(x,y,z) = x^2+y^2+z^2-2(xy+xz+yz). \tag{26}$$

Both M_t and M_l depend on the form of the interaction. For the Δ decay we take the $N\Delta\gamma$ vertex from Ref. [46]. Using this interaction we obtain the following matrix elements:

$$\begin{aligned} M_l &= (e\ f\ g)^2 \frac{m_\Delta^2}{9m_N} M^2 4(m_\Delta - m_N - q_0), \\ M_t &= (e\ f\ g)^2 \frac{m_\Delta^2}{9m_N}\left[q_o^2(5m_\Delta - 3(q_0+m_N)) \right. \\ &\quad \left. - M^2(m_\Delta + m_N + q_0)\right], \end{aligned} \tag{27}$$

with

$$f = -1.5\frac{m_\Delta + m_N}{m_N[(m_N+m_\Delta)^2 - M^2]}, \tag{28}$$

q_0 the energy of the dilepton pair in the Δ center of mass, e the electric charge, and $g = 2.72$ the coupling constant fitted to the photonic decay width $\Gamma_0(0) = 0.72$ MeV [47].

IV. THE C + C REACTION AT 2 AND 1*A* GEV

For the simulation of the heavy-ion reaction we use the IQMD program, which has been described in Sec. I. The details of this program can be found in Ref. [13].

The presented results are averaged over impact parameter and have been corrected for the experimental mass resolution and acceptance with a program provided by the HADES Collaboration. We have neglected in our calculation the reabsorption cross section of the η mesons, which is of the order of 20 mb [48] in our kinematic domain but of little importance for such a light system. We compare the results of the standard setup, where free masses and widths as well the most common extrapolations or theoretical predictions of unknown cross sections are used, with calculation in which it is assumed that the particle properties change in the medium or in which other cross-section parametrizations are applied.

Figure 6 shows the result of the standard simulation setup: $\sigma(np \to np\eta) = 2\sigma(pp \to pp\eta)$, $\sigma(np \to np\omega) = 5\sigma(pp \to pp\omega)$, $M_\omega = M_\omega^0$, and the branching ratio $\mathrm{BR}_{\eta\to e^+e^-} = 7.7 \times 10^{-5}$. It is called standard because it uses standard literature values for the unknown physical input quantities. We see that with the resolution of the HADES experiment the direct η decay would yield a visible peak, which is not present in the data. Therefore the upper limit has to be lower than that quoted by the Particle Data Group [14]. We see

TABLE I. Definition of the various parameters for the IQMD simulations.

Model	$\mathrm{BR}_{\eta\to e^+e^-}$	m_ω	$\frac{\sigma_{pn\to pn\omega}}{\sigma_{pp\to pp\omega}}$	$\frac{\sigma_{pn\to pn\eta}}{\sigma_{pp\to pp\eta}}$
A	7.7×10^{-5}	vacuum	5	2
B	7.7×10^{-6}	vacuum	1	2
C	7.7×10^{-6}	in-medium modification	5	2
D	7.7×10^{-6}	in-medium modification	5	1
E	7.7×10^{-6}	in-medium modification	1	2

TABLE II. Comparison of the average number of collisions above threshold, of the average production cross section per NN collision in CC collisions, the cross section in elementary pp and pn reactions, and the multiplicity in pp, pn, and CC collisions at a beam energy of $2A$ GeV for η and ω mesons.

Particle Collision	η			ω		
	$p+p$	$p+n$	C + C	$p+p$	$p+n$	C + C
$\langle\sqrt{s}_{\text{coll}>\text{threshold}}\rangle$	2.697	2.697	2.677	2.697	2.697	2.811
$\langle N_{\text{coll}>\text{threshold}}\rangle$	1	1	4.65	1	1	2.32
$\langle\sigma_{\text{prod}}\rangle_{\text{C+C}}(\mu\text{b})$	115	304	203	23.8	115	66.5
$\sigma_{\text{prod}}(\mu\text{b})$	175	359		4.90	24.51	
Multiplicity	3.89×10^{-3}	8.37×10^{-3}	2.25×10^{-2}	2.36×10^{-4}	5.57×10^{-4}	3.6×10^{-3}

as well that the simulations overpredict the yield in the region of the free ω mass. This confirms the result of the simulations with other programs that have been published by the HADES Collaboration [12]. In contrast, the simulations reproduce well the mass region in which the lepton pairs are coming dominantly from the η decay and from pn bremsstrahlung. If the experimentally unknown $\sigma(np \to pn\omega)$ equals $\sigma(pp \to pp\omega)$ the yield in the M_ω mass region would be strongly reduced and comes closer to experimental data, as can be seen in Fig. 7. We obtain the same level of agreement with data if we take $\sigma(np \to pn\omega) = 5\sigma(pp \to pp\omega)$ but assume in addition that the mass of the ω decreases in the medium according to Eq. (13), as indicated by the CBELSA/TAPS results [33]. This can be seen in Fig. 8. Higher statistics data would certainly improve this situation. The best agreement is obtained in simulations with $\sigma(np \to pn\omega) = \sigma(pp \to pp\omega)$ and an in-medium ω mass, as seen in Fig. 9. Therefore, without further information on $\sigma(np \to np\omega)$ heavy-ion reactions will not reveal any robust information on in-medium modifications of the ω meson.

If we assume $\sigma(np \to np\eta) = \sigma(pp \to pp\eta)$ in the region where no data on the $\sigma(np \to np\eta)$ cross section are available (only 5% of the η are produced at an energy where experimental information on this cross section is available), we underpredict slightly the yield in this mass region, as seen in Fig. 10. The experimental error bars are too large, however, to conclude more than that there are indications that if the mass of the η does not change in the medium the $\sigma(np \to np\eta)$ is larger than $\sigma(pp \to pp\eta)$ at excess energies above 100 MeV. As for the ω meson possible in-medium changes of the η meson require a detailed study of its production in the pn channel.

Figure 11 summarizes the study of the influence of the parametrization of unknown processes on the dilepton yield. If one compares the results of the different scenarios of Table I with the experimental results, we see that the standard parametrizations (model A) yield results that are not in agreement with data at dilepton invariant masses around 550 MeV and between 750 and 950 MeV. The former difference suggests that the partial width for the disintegration of the η into a dilepton pair is much smaller than the upper limit quoted by the Particle Data Group [14]. The latter discrepancy contains the interesting physics as far as in-medium particle properties are concerned. We see that even a reduced ω production cross section in the np channel (B) does not render the calculation compatible with the data. Also the assumption that the mass of the ω changes in the medium but that it is produced with the free cross section (C) overpredicts the experimental results because it shifts the surplus only to lower invariant masses. Only the combination of a lower in-medium mass and a reduction of the standard assumption on the cross section in the pn channel (E) yields results that are compatible with the experimental error bars. Scenario (D) demonstrates that the data are not sufficiently precise to allow for robust conclusions on the $np \to np\eta$ channel. A variation of a factor of 2 gives results that are compatible with experiment.

Thus the C + C data at $2A$ GeV show interesting new physics that is not compatible with the input of state-of-the-art transport codes. Unfortunately, without further information on the elementary cross sections with a neutron in the entrance channel it will not be possible to identify the origin of this discrepancy because a modification of the mass of the mesons in the medium yields the same effect as a change of the (experimentally unknown) cross section in the np channel.

By lowering the energy to $1A$ GeV the importance of the different channels changes and a comparison between the 2 and $1A$ GeV data will elucidate part of the physics. Because the experimental data are divided by the number of π^0, the spectra for the pions change very little owing to the acceptance corrections. The same is true for the Δ Dalitz decay. The yield of e^+e^- pairs from η Dalitz decay and bremsstrahlung are lower, however, and the ω production is practically absent because of the lack of energy (even if one takes into account that the Fermi momentum may create a larger $\sqrt{s}$ value than in NN collisions at the same beam energy). Figure 12 displays our filtered and acceptance-corrected results. In the intermediate mass region the Δ Dalitz decay and bremsstrahlung have gained importance and are of the same order of magnitude. Dilepton pairs from η Dalitz decay are less frequent and are no longer dominant in the intermediate mass region. At this energy about 35% of the η comes from a $\sqrt{s}$ region where the np production cross section is known. So the uncertainty in this channel is reduced but still present. In the standard simulation setup the dilepton invariant mass spectrum at intermediate masses always has a strong bremsstrahlung component, which contributes about 50% of the yield. At invariant masses of around 200 MeV the Δ Dalitz decay contributes the other 50%—if it exists.

TABLE III. Comparison of the average number of collisions above threshold, of the average production cross section per NN collision in CC collisions, the cross section in elementary pp and pn reactions, and the multiplicity in pp, pn, and CC collisions at a beam energy of $1A$ GeV for η and ω mesons.

Particle Collision	η			ω		
	$p+p$	$p+n$	C + C	$p+p$	$p+n$	C + C
$\langle\sqrt{s}_{\text{coll}>\text{threshold}}\rangle$	x	x	2.498	x	x	2.711
$N_{\text{coll}>\text{threshold}}$	x	x	0.812	x	x	0.0176
$\langle\sigma_{\text{prod}}\rangle_{\text{C+C}}$ (μb)	30.2	146.3	84.7	7.11	38.3	22.66
$\langle\sigma_{\text{prod}}\rangle$($\mu$b)	0	0		0	0	
Multiplicity	0	0	1.61×10^{-3}	0	0	8.34×10^{-6}

The data at $1A$ GeV should therefore allow us to define an upper limit of the Δ Dalitz decay. At higher invariant masses it is the η decay that contributes the other 50%. If we assume that $\sigma(np \to np\eta) = \sigma(pp \to pp\eta)$ the η yield becomes so low that its influence on the spectrum is hardly visible.

If we lower the in-medium ω mass we see a larger ω production cross section but it remains a small contribution to the total yield, as seen in Fig. 13.

It is interesting to see in detail the differences between elementary collisions at $\sqrt{s} = 2.697$ GeV and heavy-ion collisions at the same nominal energy that show the large $\sqrt{s}$ distribution of the NN collisions displayed in Fig. 14. There we see two peaks. The high-energy peak is due to collisions between projectile and target nucleons, whereas the low-energy peak is due to collisions between either projectile or target nucleons. The latter collisions contribute only to the bremsstrahlung and to the π^0 part of the dilepton spectrum. Because of rescattering the maximum of the distribution of the primary collisions is shifted toward a lower $\sqrt{s}$ value. The consequences of the broad $\sqrt{s}$ distribution on the η and ω production as compared to elementary collisions at the nominal energy are summarized in Table II. The first line shows the average $\sqrt{s}$ value of all collisions above threshold. For the η this value is slightly below the value for elementary collisions, but for the ω (because of the larger threshold) it is slightly above. Also the average number of collisions in C + C reactions depends on the particle type, as seen in the second line. For η production we find 4.65 collisions above threshold for the ω production 2.32. For the standard scenario [$m_\omega = m^0_\omega$, $\text{BR}(\eta \to e^+e^-) = 7.7 \times 10^{-5}$, $\sigma(pn \to pn\eta) = 2\sigma(pp \to pp\eta)$, and $\sigma(pn \to pn\omega) = 5\sigma(pp \to pp\omega)$], we display in the third and the fourth lines the average production cross section in np and pp collisions in the heavy-ion reaction compared to the elementary reaction. For the η the average $\sigma(pp \to pp\eta)$ and $\sigma(pn \to pn\eta)$ are lower in CC collisions than in elementary ones. This decrease has two origins: (i) the lower $\langle\sqrt{s}_{\text{coll}>\text{threshold}}\rangle$ and (ii) the form of the η production cross section, which has a maximum at around $\sqrt{s} = 2.697$ GeV and stays almost constant at higher energies. For the ω meson the situation is completely different. The elementary cross section increases with energy for all relevant energies and the average $\sqrt{s}$ value in C + C is larger than that in elementary collisions. Therefore np as well as pp collisions in the heavy-ion reaction produce more ω mesons than elementary collisions at the same nominal energy. Consequently, the enhancement factor of η and ω mesons in heavy-ion collisions is very different.

For the $1A$ GeV reaction (Table III) the situation is very different. The $\sqrt{s}$ distribution of the collision in C + C is displayed in Fig. 15. In elementary NN collisions at the same energy neither ω nor η mesons can be produced ($\sqrt{s}_{\text{threshold }\omega} = 2.659$ GeV and $\sqrt{s}_{\text{threshold }\eta} = 2.424$ GeV). However, with the Fermi momentum, in C + C collisions subthreshold ω and η production is possible. Because of the larger threshold, ω production is suppressed with respect to η production. The production cross section at this energy tests the Fermi motion in the simulations, which is not easy to model in semiclassical simulation codes. Therefore systematic errors reduce the predictive power for the meson production at this energy, but the analysis of the subthreshold kaon production shows that in between a factor of 2 the results are certainly trustworthy.

In summary we have shown that the dilepton spectrum measured by the HADES Collaboration in the reaction of C + C at $2A$ GeV and invariant masses above 600 MeV is not compatible with the standard scenario of simulation programs that use free cross sections and free meson masses. Introducing a medium modification of the ω mass and lowering the unknown $pn \to pn\omega$ cross section brings the calculation in agreement with data. The extrapolation from elementary cross section at the same nominal energy to heavy-ion reactions is all but trivial. It depends on the threshold and on the energy dependence of the cross section. We will be able to use heavy ion data to learn something on in-medium modifications of meson properties only when we will know better the elementary meson and resonance production cross sections.

ACKNOWLEDGMENTS

We acknowledge valuable discussions with M. Bleicher, R. Holzmann, W. Kühn, and J. Stroth and thank the HADES Collaboration for providing us with the filter routines. G. Wolf acknowledges partial support from Grant Nos. T48833 and T47347.

[1] N. Bianchi *et al*., Phys. Rev. C **54**, 1688 (1996); V. Muccifora *et al*., *ibid*. **60** 064616 (1999); B. Krusche and S. Schadmand, Prog. Part. Nucl. Phys. **51**, 399 (2003).
[2] M. M. Giannini and E. Santopinto, Phys. Rev. C **49**, R1258 (1994); M. Hirata, N. Katagiri, K. Ochi, and T. Takaki, *ibid*. **66**, 014612 (2002).
[3] R. Rapp and J. Wambach, Adv. Nucl. Phys. **25**, 1 (2000).
[4] C. L. Korpa and M. F. M. Lutz, Acta Phys. Hung. A **22**, 21 (2005) and references therein.
[5] C. Hartnack and J. Aichelin, J. Phys. G **30**, S531 (2004); Ch. Hartnack, nucl-th/0507002.
[6] R. J. Porter *et al*., Phys. Rev. Lett. **79**, 1229 (1997); G. Roche, Phys. Lett. **B226**, 228 (1989).
[7] D. Miskowiec, Nucl. Phys. **A774**, 43 (2006).
[8] V. L. Eletsky, M. Belkacem, P. J. Ellis, and J. I. Kapusta, Phys. Rev. C **64**, 035202 (2001).
[9] K. Gallmeister, B. Kämpfer, O. P. Pavlenko, and C. Gale Nucl. Phys. **A688**, 939 (2001).
[10] R. Arnaldi *et al*., Phys. Rev. Lett. **96**, 162302 (2006).
[11] T. Renk and J. Ruppert, hep-ph/0612113; K. Dusling and I. Zahed, hep-ph/0701253.
[12] I. Froelich *et al*., Eur. J. Phys. A **31**, 831 (2007).
[13] C. Hartnack *et al*., Eur. Phys. J. A **1**, 151 (1998).
[14] S. Eidelmann *et al*., Phys. Lett. B **592**, 1 (2004).
[15] N. M. Kroll and W. Wada, Phys. Rev. **98**, 1355 (1955).
[16] P. Moskal *et al*., Phys. Rev. C **69**, 025203 (2004).
[17] F. Balestra *et al*., Phys. Rev. C **69**, 064003 (2004).
[18] V. Flaminio, W. G. Moorhead, D. R. O. Morrison, and N. Rivoire, Compilation of cross sections III: p and $\bar{p}$ (1984).
[19] K. Nakayama, J. Speth, and T.-S. H. Lee, Phys. Rev. C **65**, 045210 (2002).
[20] H. K. Wöhri, thesis, CERN-SPS, 2004.
[21] M. T. Peña, H. Garcilazo, and D. O. Riska, Nucl. Phys. **A683**, 322 (2001).
[22] K. Nakayama, J. Speth, and T.-S. H. Lee, Phys. Rev. C **65**, 045210 (2002).
[23] S. Abd El-Samad *et al*., Phys. Lett. **B522**, 16 (2001).
[24] F. Hibou *et al*. Phys. Rev. Lett. **83**, 492 (1999).
[25] F. Balestra *et al*., Phys. Rev. C **63**, 024004 (2001).
[26] G. Wolf (private communication).
[27] K. Tsushima and K. Nakayama, Phys. Rev. C **68**, 034612 (2003).
[28] C. Fuchs, M. I. Krivoruchenko, H. L. Yadav, A. Faessler, B. V. Martemyanov, and K. Shekhter, Phys. Rev. C **67**, 025202 (2003).
[29] M. I. Krivoruchenko *et al*., Ann. Phys. (NY) **296**, 299 (2002).
[30] M. F. M. Lutz, G. Wolf, B. Friman, Nucl. Phys. **A706**, 431 (2002); **A765**, 431(E) (2006).
[31] M. Post *et al*., Nucl. Phys. **A689**, 753 (2001).
[32] K. Gallmeister *et al*., Nucl. Phys. **A782**, 166 (2007).
[33] D. Trnka *et al*., Phys. Rev. Lett. **94**, 192303 (2005).
[34] S. Barsov *et al*., Eur. Phys. J. A **21**, 521 (2004).
[35] G. Wolf, Acta. Phys. Polon. B **26**, 583 (1995).
[36] R. D. Pisarski, Phys. Rev. D **52**, R3773 (1995).
[37] G. Chanfray, R. Rapp, and J. Wambach, Phys. Rev. Lett. **76**, 368 (1996); R. Rapp, G. Chanfray, and J. Wambach, Nucl. Phys. **A617**, 472 (1997).
[38] T. Hatsuda and S. H. Lee, Phys. Rev. C **46**, R34 (1992).
[39] G. E. Brown and M. Rho, Phys. Rev. Lett. **66**, 2720 (1991); G. Q. Li, C. M. Ko, and G. E. Brown, *ibid*. **75**, 4007 (1995).
[40] G. E. Brown and M. Rho, Phys. Rep. **363**, 85 (2002).
[41] M. Naruki *et al*., Phys. Rev. Lett. **96**, 092301 (2006); K. Ozawa *et al*., *ibid*. **86**, 5019 (2001).
[42] T. Renk and J. Ruppert, hep-ph/0605130.
[43] R. Rapp *et al*., Nucl. Phys. **A782**, 275 (2007).
[44] G. J. Gounaris and J. J. Sakurai, Phys. Rev. Lett. **21**, 244 (1968).
[45] B. E. Lautrup and J. Smith, Phys. Rev. D **3**, 1122 (1971).
[46] G. Wolf, G. Batko, W. Cassing, U. Mosel, K. Niita, and M. Schäfer, Nucl. Phys. **A517**, 615 (1990).
[47] G. Wolf *et al*., Nucl. Phys. **A517**, 615 (1990).
[48] R. S. Bhalerao and L. C. Liu, Phys. Rev. Lett. **54**, 865 (1985).